Installation Effects in Geotechnical Engineering – Hicks et al. (eds)

Numerical modeling of fracturing in soil mix material

G. Van Lysebetten & A. Vervoort
KU Leuven, Leuven, Belgium

N. Denies & N. Huybrechts
Belgian Building Research Institute, Geotechnical division, Limelette, Belgium

J. Maertens
Jan Maertens BVBA, Belgium
KU Leuven, Leuven, Belgium

F. De Cock
Geotechnical Expert Office GEO.BE, Lennik, Belgium

B. Lameire
Belgian Association of Foundation Contractors ABEF, Brussels, Belgium

ABSTRACT: The deep soil mixing technique consists of an in situ mechanical mixing of the soil with an injected binder (e.g. cement). However, the presence of soil inclusions (poorly or even unmixed soil) in the artificial material is unavoidable. This heterogeneous character of soil mix material makes it different from traditional building materials. The presented research investigates the influence of the volume percentage of inclusions on the strength, stiffness, stress-strain behaviour and fracture pattern of soil mix material. 2D numerical simulations are conducted using a Discrete Element Program (UDEC) and the results are compared with experimental data. It is observed that the reduction of the strength and stiffness of a sample is significantly larger than the weighted average of the UCS and Young's modulus, taking into account the volumes of the well mixed material and the softer inclusions. However, the strength is remarkably more affected by the volume percentage of inclusions than the stiffness. Moreover, other parameters than the percentage of weak material are also important (e.g. shape, size and relative position of the inclusions) and result in wide ranges of resulting strength and stiffness.

1 INTRODUCTION

1.1 *Deep soil mixing technique*

The application of the soil mix technology in Belgium is sharply increasing (Denies et al. 2012a). Next to soil improvement applications, soil mix walls are extensively used for excavation support because of its economic and environmental advantages compared with classical techniques such as concrete secant pile walls, diaphragm walls and king post walls (i.e. soldier pile walls). The soil mix technique is based on an in situ mechanical mixing of the soil with an injected binder (e.g. cement). By executing overlapping rectangular panels or cylindrical columns a continuous wall is obtained. As soon as the panel or column has been mixed, steel H or I profiles are inserted into the fresh soil mix material to increase the shear and bending resistance of the wall. Depths up to 20 meters are currently reached.

However, since a natural material (i.e. soil) is being mixed, it is to be expected that the entire wall is not perfectly mixed and homogeneous. The volume percentage of inclusions depends on the soil type and mixing technique (e.g. 0 to 3.5% in sandy soils up to 35% and more in stiff clays (Ganne et al. 2011). This heterogeneous character makes the material different from traditional building materials. In order to formulate alternative design rules, a Flemish regional research project (IWT 080736) in collaboration with the BBRI, ABEF and KU Leuven was initiated. This paper deals with one particular aspect of the project which is the influence of the volume percentage of inclusions on the strength, stiffness, stress-strain behaviour and fracture pattern of soil mix material.

1.2 *Aim of the study*

Apart from an experimental part consisting of laboratory experiments on small scale samples as well as large blocks, complementary numerical simulations (2D) are conducted in UDEC, a numerical program based on the discrete element method. The followed approach allows simulating fracture initiation and growth in and around the soft soil inclusions. This allows a correct distinction between shear and tensile fractures, but helps also to understand and quantify the effect of heterogeneities in the studied material. A large number of simulations have been executed to study the influence of the volume percentage, shape, number and relative position of the inclusions.

1.3 *Advantage of discrete simulations*

During the past decades, several numerical approaches have been elaborated to realize the simulation of crack initiation and propagation. Some of these codes are based on finite elements, on finite differences or on displacement discontinuity boundary elements. Though, it is found that the Distinct Element Method (DEM) is a more than valuable alternative (Debecker et al. 2006). Several DEM codes have been developed. In the Particle Flow Code (PFC) materials are modeled as a dense packing of rigid spherical elements, bonded together at their contact points (Potyondy & Cundall 2004). For this study, the Universal Distinct Element Code (UDEC) is chosen. This code is originally developed for the simulation of fractured rock mass behavior, e.g. slope stability and rock fall which depend on the activation of existing fractures (Itasca 2004). However, in the past it has been successfully used for the numerical modeling of fracture initiation and growth in rock (Debecker 2009, Tempone & Lavrov 2008).

2 NUMERICAL SIMULATIONS

2.1 *Concept and global approach*

UDEC is a 2D numerical program that is based on the discrete element method (Cundall 1971). The discrete element model consists of discrete blocks that are mutually connected by contacts. For these contacts tensile and shear failure criteria are defined, allowing them to open and deform upon activation. The UDEC solution scheme is based on a (dynamic) explicit finite-difference method which is also used in continuum analysis (Cundall & Board 1988).

The philosophy followed in this study is that by dividing a medium in multiple discrete small blocks (tightly bounded together), their boundaries can act as potential fracture paths when an external load is applied (Debecker 2009, Vervoort et al. 2012). Or in other words, a contact between two adjacent blocks does not represent a physical crack as long as it is not activated. An example of a mesh of triangles for a rectangular medium is shown in Figure 1a. Since fracture growth is limited to the available contacts, the distribution of the contacts should be as uniformly as possible so that there is no bias by the mesh. Moreover, on a larger scale a given fracture with a certain overall direction tends to develop as a combination of activated individual contacts with sometimes very different orientations, as illustrated in Figures 1b and 1c for a 60° inclined crack.

In this study, the blocks only deform elastically. The strength parameters of the material are thus not explicitly implemented in the blocks. However, the contacts are modelled with a Mohr-Coulomb failure criterion with tension cut-off. After activation, the strength parameters are set to residual values. In addition to this, UDEC models the contacts with stiffness, in shear and normal direction (respectively k_s and k_n). This stiffness allows deformation of contacts prior to activation. The deformation due to this contact stiffness has an effect on the stress distribution within the sample (Debecker et al. 2006).

2.2 *Calibration of model parameters*

On the one hand, material properties as obtained from laboratory tests are assigned to the triangular blocks (Table 1). On the other hand, the stiffness and strength parameters of the contacts are not physically measurable and their values are deduced from a calibration process. First, the contact properties for a homogeneous model of well mixed material are calibrated based on the stress-strain behavior and typical fracture patterns during uniaxial compression tests. These properties are all well-known from laboratory tests (e.g. peak strength, Young's modulus, post-peak behavior,

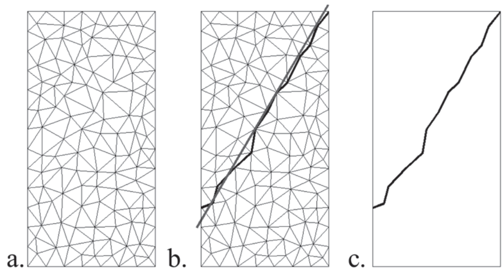

Figure 1. (a) Simplified example of adjacent triangular blocks that form the sample. A contact only represents a physical crack when it is activated. (b) Fracture along activated contacts with a global dip of 60° (straight line). (c) Apart from the activated contacts the sample is still intact.

Table 1. Material properties of the blocks corresponding to the matrix material and the soft inclusions (Van Lysebetten 2011).

Material properties	Matrix	Inclusions
Density ρ [kg/m³]	1820	1820
Young's modulus E [GPa]	11.6	0.165
Poisson's ratio υ [–]	0.3	0.4
Bulk modulus K [GPa]	9.67	0.275
Shear modulus G [GPa]	4.46	0.059

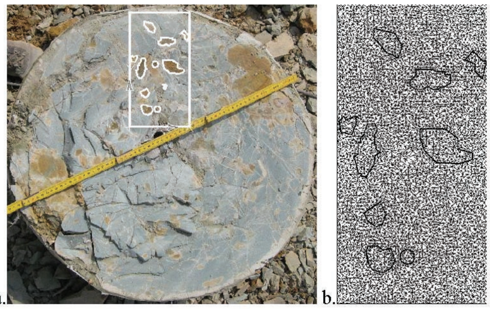

a. b.

Figure 2. (a) 2D sample (120 × 240 mm) from a real soil mix column cross-section. (b) Mesh of the basic model.

failure by 60 to 70° inclined shear fractures, etc.). This time-consuming process finally leads to the matrix—matrix contact strength and stiffness parameters. Next, the strength properties of matrix—inclusion and inclusion—inclusion contacts are easily deduced from the matrix—matrix contact strength by applying the strength ratios of mixed and unmixed material.

2.3 *Basic model*

The starting point for the soil mix samples is a section through a real soil mix column, of which an area of 120 × 240 mm is considered (Fig. 2a). This 2D sample contains 11 inclusions which account for 11 vol%. Based on this sample, the basic model is assembled. It consists of 9 of the 11 inclusions or 10 vol% of inclusions (Fig. 2b). Note that the term vol% is justified, since the 2D model in fact has a unit thickness. Moreover, using this terminology the link with the measurements on real soil mix material is more easily made.

2.4 *Mesh generation algorithm*

As illustrated by the basic model in Figure 2b, the mesh of a soil mix sample is built up by a combination of a predefined structure and a certain degree of randomness. Or in other words, the predefined shape and location of the inclusions are incorporated in a (random) mesh of triangles. Since UDEC does not provide a mesh generator that can meet these requirements, a mesh generator was implemented in Matlab. The algorithm divides the sample in multiple small rectangular sectors in which grid nodes are randomly generated around the predefined nodes of the inclusions. Finally, Delaunay triangulation is performed on the entire collection of nodes (i.e. nodes that define the boundary of the inclusions as well as the randomly generated nodes). The triangulation algorithm is based on the Quickhull algorithm for constructing convex hulls (Barber et al. 1996). To keep calculation time in UDEC reasonable, the number of triangles is limited to approximately 8000. Of course, this limits the minimal representative length of the individual contacts of the discrete model and consequently the minimum fracture length that can be simulated (Debecker & Vervoort 2006). The quality of the generated mesh is largely dependent on the choice of the input parameters, such as the minimum distance between grid nodes in relation to the dimensions of the sectors.

An appropriate mesh for fracture simulation must meet several geometrical requirements. First, the boundary of the inclusions must be respected by the edges of the generated triangles (the edges are called 'elements' from now on). Second, the distribution of the element orientation should be as uniformly as possible, as discussed in paragraph 2.1. Third, adjacent triangles should be of approximately the same size and sharp triangles should be avoided, both to guarantee reasonable solution accuracy in UDEC. In order to check the generated triangles, quality parameters have been introduced (Debecker & Vervoort 2006):

- 'Minimum triangle angle': the smallest angle of the triangle and a degree to evaluate the skinniness of the triangles. Its aimed interval is [20°, 60°].
- 'Triangle aspect ratio': a measure for the maximum edge size to the minimum altitude of the triangle. Its ideal interval is [1, 2.5].
- 'Triangle quality' Q: the ratio of the smallest angle to the largest angle of the triangle. The ideal interval of Q is [0.4, 0.9].

The present algorithm provides an overview of all quality parameters after the mesh has been generated. Note that all quality parameters are only indicative and not stringent.

2.5 *Results of the simulations*

In order to study the influence of several inclusion properties (e.g. vol%, shape, size, relative position), about 200 uniaxial compression tests on soil mix models (120 × 240 mm) with different inclusion geometries have been simulated.

2.5.1 *Influence of volume percentage, shape and size of the inclusions*

On the basis of the real 2D section and the basic model (Figs. 2a and 2b), 68 additional models are generated with 1, 5, 10 and 20 vol% inclusions. For these models, the relative position of the inclusions is varied as well as the shape (e.g. explicitly rounded or sharp-ended) and the number of inclusions (e.g. 1 large rounded inclusion against 3 smaller rounded inclusions).

The evolution of the fracture pattern of the basic model (Fig. 2b) is presented in Figures 3a, b and c for 3 different loading steps (just before, at and just after peak strength). The basic model has a UCS value of 4.4 MPa against a UCS value of 11.7 MPa for the pure soil mix sample without inclusions. The 9 inclusions (a total of 10 vol%) reduce the strength thus with more than 60%. At relatively low vertical loads (less than 50% of the peak strength) a part of the material inside the inclusions starts to fail. This is logical since the inclusions have lower strength properties. However, failure is clearly limited to specific parts of the inclusions. At 2.6 MPa vertical load several vertical splitting type of fractures are induced in the matrix at the top and at the bottom of the grouped inclusions (Fig. 3a). At higher vertical loads, especially after the UCS value has been reached (Fig. 3b), also shear fractures are induced. Finally, this results in a shear zone that extends from the upper left corner to the lower right corner of the sample (Fig. 3c).

Figure 3d presents three detailed fracture patterns of tested samples, cored from a real soil mix wall with several soil inclusions. The inclusions are clearly visible, as well as the induced fractures. Moreover, the observed fractures are comparable to the simulated fracture patterns around inclusions. For example in the left picture, two fractures are induced at both extremities of the bottom part of the inclusion, which is also observed around several inclusions in the simulations. In the central and right pictures, fractures are observed somewhere along the middle of the inclusion or at the most top or bottom point of the inclusion. Again, these fractures are also visible in the simulations.

Figure 4 compares laboratory data of in situ cored samples from 12 different Belgian construction sites with the results of the numerical simulations (69 models). Both sets of results show a similar downward trend in function of the volume percentage of inclusions. The results of the simulations are clearly situated within the (wider) range of laboratory results. The fact that the experimental data have a wider range is logical, as the soil type at the 12 constructions sites is different. Clayey, as well as loamy and sandy soils were encountered, and of course the mechanical characteristics of the different soil mix materials are different (Denies et al. 2012b). For the numerical simulations one single value is considered for the model without any inclusions, i.e. a strength value of 11.7 MPa for the homogeneous sample. Other reasons for the wider range are that in reality a real soil mix sample is never perfectly homogeneous

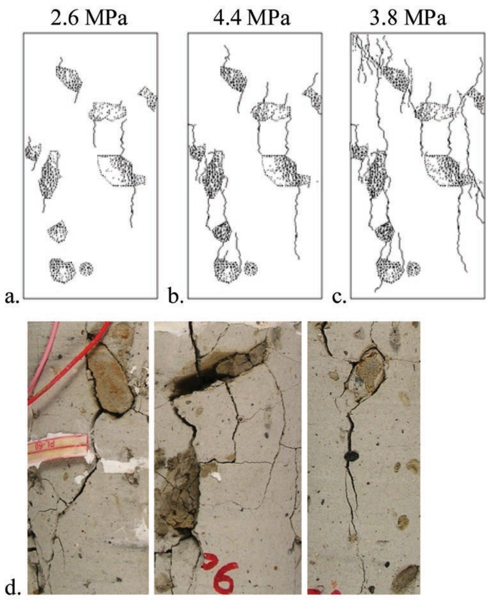

Figure 3. (a, b, c) Evolution of the fracture pattern of the basic model. (d) Examples of real fracture patterns of uniaxial loaded soil mix samples.

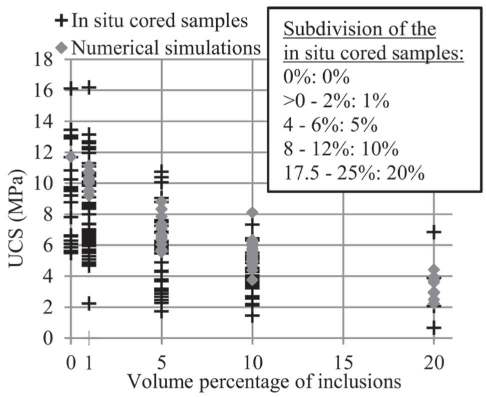

Figure 4. Comparison of the variation of strength (UCS) in function of the volume percentage of unmixed material for the numerical simulations (results based on Van Lysebetten (2011)) and for the results of laboratory experiments.

and that two samples even without any inclusions (or with exactly the same amount of inclusions) still have different strength values because of variations in e.g. cement content.

Therefore, the numerical simulations are more suitable to study the effect of the volume percentage of unmixed material on the strength of a sample. The numerical results of Figure 4 are based on the basic model and the 68 additional models (diamond-shaped markers). First, the decrease of strength is clearly larger than the percentage of inclusions in the sample. For a mere 1% of unmixed material strength is reduced by 13% on average. For 10% of inclusions even half of the strength disappears on average (Van Lysebetten 2011). The same can be concluded for the stiffness (Vervoort et al. 2012), though it is less influenced (for 1 and 10 vol% of inclusions the stiffness is reduced on average with respectively 3 and 32%). Second, there is an overlapping zone between the strengths of 5 and 10% and of 10 and 20%. This overlap is caused by the relatively large range for each volume percentage of inclusions. For the stiffness, there is just no overlap between successive volume percentages.

Strength and stiffness of a sample are clearly not only determined by the volume percentage. This is further analyzed for additional models with 10% of inclusions. It is observed that strength and stiffness are reduced more by sharp-ended inclusions than by rounded inclusions. Apart from this, the strength of a sample also drastically decreases when less inclusions (but with the same shape and the same total percentage of inclusions) are present (Vervoort et al. 2012).

2.5.2 *Influence of the relative position of the inclusions*

Apart from the volume percentage, size and number of inclusions, the relative position has also an influence on strength and stiffness. 123 additional models are generated to study this effect. All additional models represent 10% of inclusions and are composed of two sets of respectively 3 and 5 inclusions. The main difference between all models is the relative position of these inclusions. In some models, they are concentrated, in others they are spread as wide as possible, or they are nicely situated along a vertical line or along a diagonal, etc. The ranges of strength (3.8–8.1 MPa) and stiffness (5–8.7 GPa) increase in comparison with the results of the 69 models for the study of the influence of the volume percentage, shape and number of inclusions (respectively 3.1–9.2 MPa and 6.3–7.9 GPa). This is logical since the more simulations, the greater the probability that new minimum and maximum values are found.

The simulations clearly show the influence of the relative position of the inclusions on the strength and stiffness of a sample (Van Lysebetten et al. 2012). For example, it is observed that strength and stiffness decrease if the inclusions are located along the diagonal of the sample. This configuration probably facilitates a global shear failure. Figure 5a shows that there is a clear negative trend between strength and stiffness and $w_{i/t}$: the ratio of the total width of inclusions, i, and the sample width, t (Fig. 5b). However, a significant overlap is also observed, e.g. the largest UCS value for a width ratio of 60% is still larger than the smallest value for 20% ratio. For the stiffness, the overlap is probably even larger. In these additional simulations, it was also observed that the strength and stiffness also decrease if the vertical distance between the inclusions decreases, since inclusions tend to act as one larger inclusion. However, this effect is less important than the influence of the ratio $w_{i/t}$.

2.5.3 *Link with simulated fracture patterns*

Figs 6a, b, c and d show the evolution of the fracture pattern of 4 models for successive loading steps. At relative low stress levels (less than 50% of the strength) vertical extension type of fractures initiate at the lower and upper parts of the inclusions (see also Figs 3a, b and c for the evolution of the fracture pattern of the basic model). Only at stress levels near the UCS value of the sample, shear fractures are observed at the sides of the inclusions after which the sample finally fails due to a combination of shear and extension type of fractures.

Most of the described effects of inclusions can be related to and explained by the observed fracture patterns. For example, stress peaks near sharp-ended inclusions are higher than close to rounded inclusions, causing fracture initiation at lower

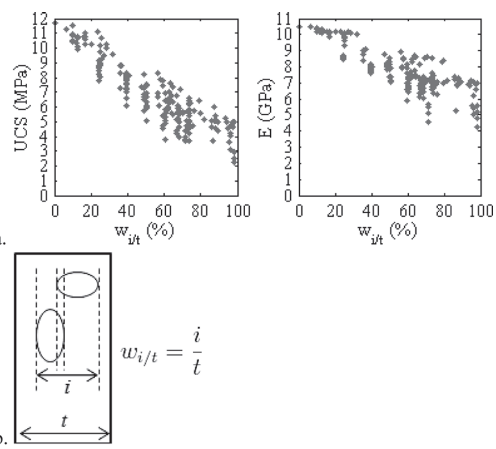

a.

b.

Figure 5. (a) Relation between the strength (left) and stiffness (right) and $w_{i/t}$. (b) Definition of the ratio $w_{i/t} = i/t$.

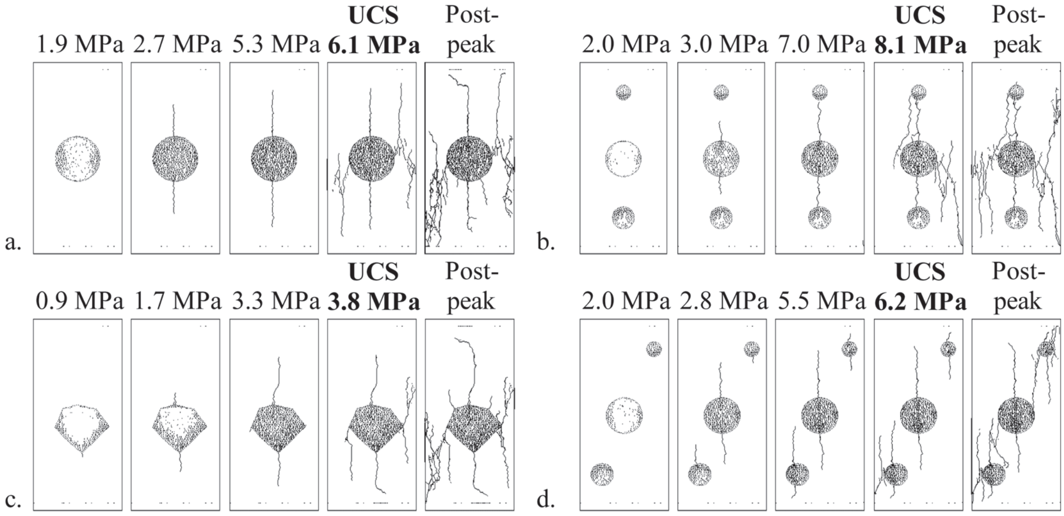

Figure 6. Illustration of the fracture pattern at successive loading steps of 4 samples of the original set each with 10% of inclusions. Shape and number of inclusions are different. The stiffness of the models is respectively 7.2 GPa, 8.0 GPa, 6.7 GPa and 7.4 GPa.

stress levels. Finally, this results in lower strength and stiffness (compare Figs 6a and c). Fracturing also initiates at lower stress levels when 1 large inclusion is present instead of 3 smaller inclusions, at least if these 3 inclusions are vertically aligned (compare Figs 6a, b and d). Again, this is caused by higher stress peaks near the largest inclusions (i.e. because a higher horizontal distance has to be bridged).

However, the fact that the 3 inclusions are vertically aligned is very important. Figure 6d shows the fracture pattern of a sample with the same 3 inclusions positioned diagonally. This sample results in about the same strength and stiffness as the sample with 1 large rounded inclusion. The large reduction of strength in comparison with the model with 3 vertically aligned inclusions is caused by the diagonal orientation of the inclusions resulting in a larger $w_{i/t}$ ratio. Moreover, the stress peaks around the stress relieved zones interfere and probably amplify each other.

Finally, if the vertical spacing between the inclusions of Figure 6b is decreased, the inclusions tend to form one larger inclusion. Overlapping zones with increased stresses expand again and the amplifying effect grows. This causes earlier fracture initiation (at lower vertical loads), but the vertical extension type fractures around the central inclusion also reach faster the upper and lower inclusions. The travelled distance through the stronger material before reaching other weak inclusions is thus lower. Because propagation through these inclusions goes much faster, a much larger part of the sample is damaged. Again, this results in lower strength and stiffness.

3 CONCLUSIONS

Although calibration of the numerical discrete model is very time-consuming, the results show that numerical simulations are very interesting to perform relatively easily sensitivity analyses. The influence of soil inclusions on the strength and stiffness of soil mix material has been investigated by a total of 192 simulations. It has been observed that soft inclusions have a large impact on the resulting strength and stiffness of a sample. However, not only the volume percentage is important, but also the relative position of the inclusions, their shape and number, etc. Moreover, UDEC has shown to be suitable for the simulation of fracture initiation and growth in soil mix material with soft inclusions. Similar trends of the influence of the volume percentage of inclusions on the strength are observed for the results of laboratory data of in situ cored samples from different Belgian construction sites and the results of numerical simulations. The simulated fracture patterns are also comparable with these observed in real soil mix samples.

ACKNOWLEDGEMENTS

This project has been made possible by the financial support of the Flemish government agency for

Innovation by Science and Technology (IWT). It is the result of cooperation between the Belgian Building Research Institute (BBRI), the Belgian Association of Foundation Contractors (ABEF) and KU Leuven.

REFERENCES

Barber, C.B., Dobkin, D.P, Huhdanpaa, H. 1996. The Quickhull algorithm for convex hulls. *ACM Transactions on Mathematical Software*, Vol. 22 (4), pp. 469–483.

Cundall P.A. 1971. A computer model for simulating progressive large scale movements in block rock systems. *Proceedings of the International Society for Rock Mechanics Symposium*, paper II-8.

Cundall P.A. & Board M. 1988. A microcomputer program for modeling large-strain plasticity problems. *Proceedings of the 6th International Conference on Numerical Methods in Geomechanics. Rotterdam (Netherlands)*, pp. 2101–2108.

Debecker B. 2009. Influence of planar heterogeneities on the fracture behavior of rock, *Ph.D. Dissertation, KU Leuven, Leuven (Belgium).*

Debecker B., Vervoort A., Napier J.A.L. 2006. Fracturing in and around a natural discontinuity in rock: a comparison between boundary and discrete element models. *Proceedings* of the 5th International Conference on Engineering Computational Technology, Las Palmas de Gran Canaria (Spain), paper 168.

Debecker B. & Vervoort A. 2006. A 2D triangular Delaunay grid generator for the simulation of rock features. Proceedings of the 5th International Conference on Engineering Computational Technology, Las Palmas de Gran Canaria (Spain), paper 220.

Denies N., Huybrechts N., De Cock F., Lameire B., Maertens J., Vervoort A. 2012a. Soil mix walls as retaining structures, Belgian practice. *Proceedings of TC211 International Symposium on Ground Improvement, Brussels (Belgium),* Vol. 3, pp 83–97.

Denies N., Huybrechts N., De Cock F., Lameire B., Vervoort A., Maertens J. 2012b. Soil mix walls as retaining structures, mechanical characterization. *Proceedings of the TC 211 International Symposium on Ground Improvement, Brussels (Belgium)*, Vol. 3, pp. 99–115.

Ganne P., Denies N., Huybrechts N., Vervoort A., Tavallali A., Maertens J., Lameire B., De Cock F. 2011. Soil Mix: influence of soil inclusions on the structural behavior. *Proceedings of the 15th European conference on soil mechanics and geotechnical engineering, Athens (Greece)*, pp. 977–982.

Itasca 2004. UDEC v4.0 manual. Itasca Consulting Group, Inc., Minnesota, USA.

Potyondy D.O. & Cundall P.A. 2004. A Bonded-Particle Model for Rock. *International Journal for Rock Mechanics & Mineral Sciences*, Vol. 41(8), pp. 1329–1364.

Tempone P. & Lavrov A. 2008. DEM modeling of mud-losses into single fractures and fracture networks. Proceedings of the 12th international conference of the international association for computer methods and advances in geomechanics, Goa (India), pp. 2475–2482.

Van Lysebetten G., Vervoort A., Maertens J., Huybrechts N. 2012. Discrete modelling for the study of the effect of soft inclusions on the behaviour of soil mix material. *In preparation.*

Van Lysebetten G. 2011. Soil Mix for Construction purposes: Quality control. *M.Sc. Thesis (Geotechnical and Mining Engineering) KU Leuven, Leuven.*

Vervoort A., Van Lysebetten G., Tavallali A. 2012. Numerical modeling of fracturing around soft inclusions. *Proceedings of the Southern Hemisphere International Rock Mechanics Symposium, Sun City (South-Africa)*, pp. 33–46.